A novel form of synaptic plasticity in field CA3 of hippocampus requires GPER1 activation and BDNF release

Victor Briz,[1,3] Yan Liu,[1,2] Guoqi Zhu,[1,4] Xiaoning Bi,[2] and Michel Baudry[1]

[1]Graduate College of Biomedical Sciences and [2]College of Osteopathic Medicine of the Pacific, Western University of Health Sciences, Pomona, CA 91766
[3]VIB Center for the Biology of Disease, Katholieke Universiteit Leuven, 3000 Leuven, Belgium
[4]Key Laboratory of Xin'an Medicine, Ministry of Education, Anhui University of Traditional Chinese Medicine, Hefei 230038, China

Estrogen is an important modulator of hippocampal synaptic plasticity and memory consolidation through its rapid action on membrane-associated receptors. Here, we found that both estradiol and the G-protein–coupled estrogen receptor 1 (GPER1) specific agonist G1 rapidly induce brain-derived neurotrophic factor (BDNF) release, leading to transient stimulation of activity-regulated cytoskeleton-associated (Arc) protein translation and GluA1-containing AMPA receptor internalization in field CA3 of hippocampus. We also show that type-I metabotropic glutamate receptor (mGluR) activation does not induce Arc translation nor long-term depression (LTD) at the mossy fiber pathway, as opposed to its effects in CA1, and it only triggers LTD after GPER1 stimulation. Furthermore, this form of mGluR-dependent LTD is associated with ubiquitination and proteasome-mediated degradation of GluA1, and is prevented by proteasome inhibition. Overall, our study identifies a novel mechanism by which estrogen and BDNF regulate hippocampal synaptic plasticity in the adult brain.

Introduction

Estrogen regulates important brain functions including learning, memory, and social behavior, and is neuroprotective against a variety of insults. Since the discovery that 17β-estradiol (E_2) modulates spine density in hippocampus (Woolley et al., 1990), many studies have addressed the mechanisms by which estrogen modulates hippocampal synaptic plasticity. It is now widely accepted that rapid nongenomic actions underlie the positive effects of estrogen on cognition (Luine, 2008; Srivastava et al., 2013). In addition, both estrogen receptor α (ERα) and β (ERβ), as well as the G-protein–coupled estrogen receptor 1 (GPER1), have been implicated in E_2-mediated cognitive enhancement (Boulware et al., 2013; Ervin et al., 2013; Hawley et al., 2014).

GPER1 mediates some of the nongenomic responses to E_2 in nonneuronal cells as well as in neurons (Prossnitz et al., 2008; Srivastava and Evans, 2013). This novel ER is broadly expressed in rat brain, including in hippocampus (Brailoiu et al., 2007; Matsuda et al., 2008), where it regulates several neuronal functions, such as neurotransmitter release and neuroprotection (Gingerich et al., 2010; Hammond et al., 2011). While the subcellular localization of GPER1 has remained controversial (Srivastava and Evans, 2013), recent ultrastructural analyses have identified GPER1 in hippocampal dendritic spines and axon terminals (Akama et al., 2013; Waters et al., 2015), which suggests its involvement in synaptic plasticity. In this regard, we recently reported that E_2-induced activation of the mechanistic target of rapamycin (mTOR) in hippocampal neurons is mediated by GPER1 (Briz and Baudry, 2014), an event required for estrogen regulation of memory consolidation (Fortress et al., 2013). Yet, the role of GPER1 activation in hippocampal synaptic plasticity is still poorly understood.

Estrogen facilitates the consolidation of long-term potentiation (LTP) in the CA1 area of hippocampus via increasing AMPA receptor–mediated synaptic transmission and inducing actin cytoskeleton reorganization (Kramár et al., 2009; Zadran et al., 2009). Furthermore, locally produced E_2 plays a crucial role in estrogen-mediated facilitation of LTP in this region (Grassi et al., 2011; Fester and Rune, 2015). Although the mechanisms by which E_2 regulates synaptic plasticity in CA1 have been extensively studied, less attention has been paid to its effects in other hippocampal areas, such as CA3 or dentate gyrus (DG). Likewise, E_2 modulates different forms of long-term depression (LTD) in hippocampus (Shiroma et al., 2005; Mukai et al., 2007; Murakami et al., 2015), but the underlying mechanism remains largely unknown.

Correspondence to Michel Baudry: mbaudry@westernu.edu

Abbreviations used in this paper: ANOVA, analyses of variance; BDNF, brain-derived neurotrophic factor; DG, dentate gyrus; ERα, estrogen receptor α; ERβ, estrogen receptor β; fEPSP, field excitatory postsynaptic potential; LTD, long-term depression; LTP, long-term potentiation; mGluR, metabotropic glutamate receptor; mTOR, mechanistic target of rapamycin; UPS, ubiquitin–proteasome system.

The Rockefeller University Press $30.00
J. Cell Biol. Vol. 210 No. 7 1225–1237
www.jcb.org/cgi/doi/10.1083/jcb.201504092

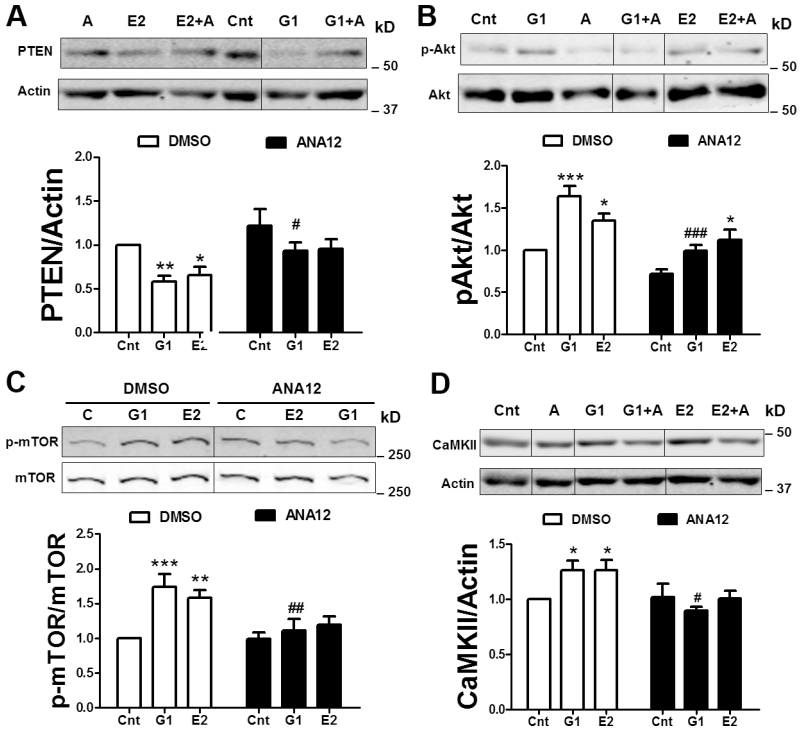

Figure 1. **G1-induced stimulation of mTOR signaling requires TrkB receptor activation.** Hippocampal slices were preincubated with DMSO or ANA-12 (50 µM) for 30 min and then treated with G1 or E2 for an additional 30 min. At the end of treatments, samples were homogenized and processed for Western blotting. Data are presented as the ratio (fold of control) of: (A) PTEN over actin (n = 4–10), (B) phospho-Akt (p-Akt) over total Akt (n = 3–8), (C) phospho-mTOR (p-mTOR) over total mTOR (n = 4–7), and (D) αCaMKII over actin (n = 4–18). *, P < 0.05; **, P < 0.01; ***, P < 0.001, as compared with control; #, P < 0.05; ##, P < 0.01; ###, P < 0.001, as compared with G1 or E2 alone (one- or two-way ANOVA). Some of the actin bands in both A and C look very similar because they show the same data. Images in these two panels come from the same blot, in which different primary and secondary antibodies were used. Thus, the same actin blot serves as loading control for both PTEN and CamKII. They have been separated into two panels for consistency in figure formatting. Black lines indicate that intervening lanes have been spliced out. Error bars indicate means ± SEM.

Type-I metabotropic glutamate receptor (mGluR) activation at CA3-CA1 Schaffer-collateral synapses elicits a form of LTD (mGluR-LTD), which requires local synthesis of the activity-regulated cytoskeleton-associated protein (Arc) and synaptic removal of GluA1-containing AMPA receptors (Waung et al., 2008). However, whether a similar phenomenon occurs at the mossy fiber–CA3 pathway is currently unknown. The present study was designed to investigate the molecular mechanisms underlying mGluR-LTD in field CA3 of the hippocampus and its modulation by estrogen. We found that E_2-induced activation of GPER1 is necessary for mGluR-LTD in the CA3 area of hippocampus, through a mechanism involving brain-derived neurotrophic factor (BDNF) release, mTOR-dependent Arc synthesis, and proteasome-mediated GluA1 degradation. Thus, our study identified a novel mechanism by which estrogen regulates synaptic plasticity in adult hippocampus.

Results

GPER1 activation stimulates mTOR signaling through BDNF release

We recently reported that estrogen-induced mTOR phosphorylation is mediated by GPER1 activation and is also blocked by the TrkB receptor antagonist K252 (Briz and Baudry, 2014). However, K252 is a nonselective protein kinase inhibitor, acting on protein kinase A, C, and G, among others (Kase et al., 1987; Rüegg and Burgess, 1989). To verify that the effects of estrogen on mTOR signaling require TrkB receptor activation, we used the novel and specific TrkB receptor antagonist ANA12 (Cazorla et al., 2011). Activation of mTOR by estrogen in hippocampal slices also involves PTEN degradation and subsequent Akt phosphorylation (Briz and Baudry, 2014). Thus, we first tested whether the GPER1 agonist G1 was able to reproduce the effects of estrogen on mTOR signaling. Treatment with either E_2 (10 nM) or G1 (100 nM) for 30 min significantly reduced PTEN levels, and stimulated Akt and mTOR phosphorylation (Fig. 1, A–C). In addition, both G1 and E_2 produced a slight but significant increase in αCaMKII levels (Fig. 1 D), a protein rapidly translated in response to synaptic activity (Roberts et al., 1996; Aakalu et al., 2001). Pretreatment with ANA12 (50 µM) blocked G1- and E_2-induced PTEN degradation. Likewise, ANA12 prevented the increase in mTOR phosphorylation and in αCaMKII levels induced by G1 and E_2. In contrast, while ANA12 completely suppressed Akt phosphorylation caused by G1, it only partially reduced E_2-induced Akt phosphorylation (Fig. 1). This is not surprising since E_2-induced Akt activation in rat hippocampus can be mediated by stimulation of both ERα and ERβ, in addition to GPER1 (Spencer-Segal et al., 2012; Ruiz-Palmero et al., 2013).

The above results confirmed that estrogen-mediated stimulation of mTOR signaling requires TrkB receptor activation. However, it is not clear whether this effect involves transactivation of the receptor (Kramár et al., 2013) or stimulation of BDNF release (Sato et al., 2007). To address this question, we used a recombinant fusion protein TrkB-Fc, which acts as a non-cell-permeable BDNF scavenger trapping endogenous BDNF released in the extracellular medium (Jourdi et al., 2009). As expected, G1 stimulated mTOR signaling in control slices incubated with IgG-Fc (Fig. 2). In contrast, preincubation of hippocampal slices with TrkB-Fc (2 µg/ml, 1 h) totally suppressed G1-induced PTEN degradation (Fig. 2 A), as well as an increase in Akt and mTOR phosphorylation (Fig. 2, B and C). Likewise, G1-induced increase in αCaMKII levels was absent in the presence of TrkB-Fc (Fig. 2 D).

To confirm that GPER1 activation triggers BDNF release, we quantified by immunoblotting the amount of BDNF released in the extracellular medium from cultured neurons. Mature cortical neurons were first incubated with TrkB-Fc (2 µg/ml, 1 h), and subsequently treated with G1 and E_2 for 1 h. Treatment with either G1 or E_2 significantly increased the levels of both BDNF monomers and homodimers (18 and 27 kD, respectively) in the

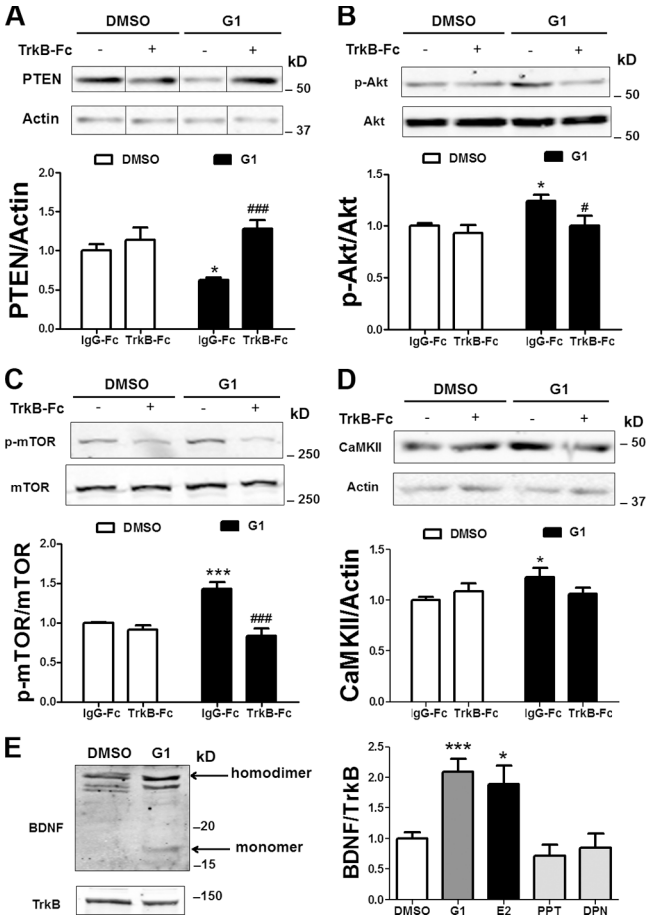

Figure 2. **G1-induced activation of mTOR signaling involves BDNF release.** (A–D) Hippocampal slices were preincubated with IgG-Fc or TrkB-Fc for 1 h and then treated with G1 for an additional 30 min. At the end of treatments, samples were homogenized and processed for Western blotting. Data are presented as the ratio (fold of control) of: (A) PTEN over actin (n = 10–12), (B) phospho-Akt (p-Akt) over total Akt (n = 11–13), (C) phospho-mTOR (p-mTOR) over total mTOR (n = 9–14), and (D) αCaMKII over actin (n = 13–16). (E) Primary cortical neurons were preincubated with TrkB-Fc for 1 h and then treated with G1, E_2, PPT, or DPN for an additional 60 min. The incubation medium was collected, concentrated, and processed for Western blotting. BDNF over TrkB (n = 4–8) is shown. *, $P < 0.05$; **, $P < 0.01$; ***, $P < 0.001$, as compared with control. #, $P < 0.05$; ##, $P < 0.01$; ###, $P < 0.001$, as compared with G1 alone (one- or two-way ANOVA). Black lines indicate that intervening lanes have been spliced out. Error bars indicate means ± SEM.

extracellular medium, as compared with control (Fig. 2 F), confirming that GPER1 activation rapidly stimulates BDNF release in neurons. In contrast, neither the ERα nor the ERβ agonist (PPT and DPN, respectively) induced BDNF release from cultured neurons (Fig. 2 F).

GPER1 activation stimulates Arc synthesis and GluA1 internalization in CA3 through a BDNF- and mTOR-dependent mechanism

As mentioned earlier, both E_2 and G1 rapidly increased (within 30 min) αCaMKII levels in hippocampal slices. To confirm that GPER1 mediated the effects of E_2 on αCaMKII synthesis, we treated slices with E_2 in the presence of a novel and very specific GPER1 antagonist, G36 (Dennis et al., 2011). Similar to its inhibitory effects on E_2-induced mTOR phosphorylation reported previously (Briz and Baudry, 2014), preincubation

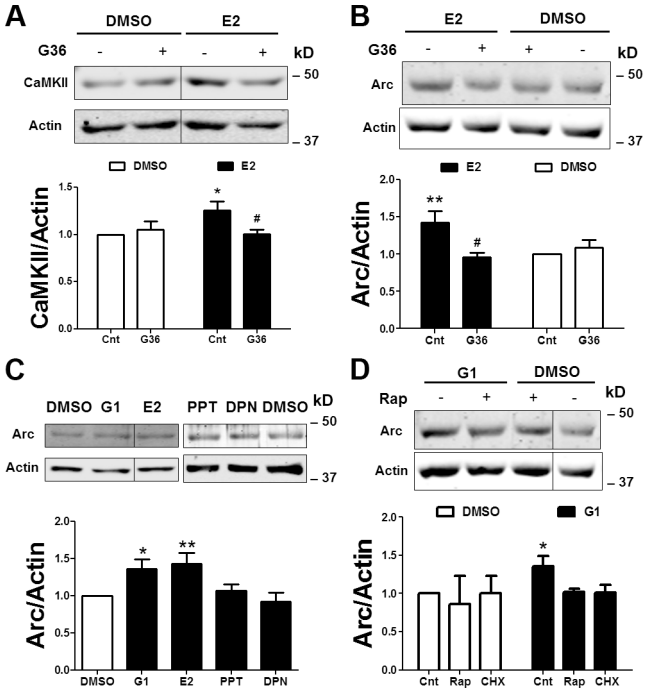

Figure 3. **Estrogen stimulates mTOR-dependent protein synthesis via GPER1 activation.** Hippocampal slices were pretreated with DMSO, G36, cycloheximide, or rapamycin for 30 min and then incubated with G1 or E_2 for an additional 30–60 min. Treatments with PPT (100 nM) or DPN (10 nM) were for 1 h. At the end of treatments, samples were homogenized and processed for Western blotting before (A) or after (B–D) membrane fractionation. Data are presented as the ratio (fold of control) of αCaMKII over actin (A; n = 5–12) or Arc over actin (B–D; n = 3–14). *, $P < 0.05$; **, $P < 0.01$, as compared with control. #, $P < 0.05$ as compared with E_2 alone (one- or two-way ANOVA). Black lines indicate that intervening lanes have been spliced out. Error bars indicate means ± SEM.

of hippocampal slices with G36 (1 μM) completely abrogated the increase in αCaMKII levels produced by E_2 (Fig. 3 A). To further investigate the significance of estrogen regulation of mTOR-dependent protein synthesis, we analyzed changes in the levels of Arc, which is rapidly synthesized in response to synaptic activity and to E_2 treatment (Chamniansawat and Chongthammakun, 2009; Kühnle et al., 2013; Briz and Baudry, 2014). However, we did not detect any significant changes in Arc levels by immunoblotting after treatment with G1 (Fig. S1 C) in homogenates of whole hippocampal slices. Because Arc has been shown to be locally translated in dendrites (Steward et al., 1998; Waung et al., 2008), we analyzed Arc levels in P2 fractions under the same experimental conditions. In this case, treatment with either G1 or E_2 significantly increased Arc levels in P2 fractions. In contrast, neither PPT nor DPN affected Arc levels in this fraction (Fig. 3 C). Consistent with this result, the effects of E_2 on Arc levels were totally suppressed by preincubation with G36 (Fig. 3 B). Furthermore, the increase in membrane Arc levels produced by G1 treatment was suppressed by the protein synthesis inhibitors cycloheximide (25 μM) and rapamycin (1 μM; Fig. 3 D). Collectively, these results indicate that E_2-induced GPER1 activation stimulates Arc and αCaMKII synthesis through a BDNF- and mTOR-dependent mechanism.

We further investigated estrogen modulation of Arc synthesis in hippocampal slices by immunohistochemistry. Under control conditions, Arc expression was found predominantly in the cell body layer of pyramidal neurons (especially

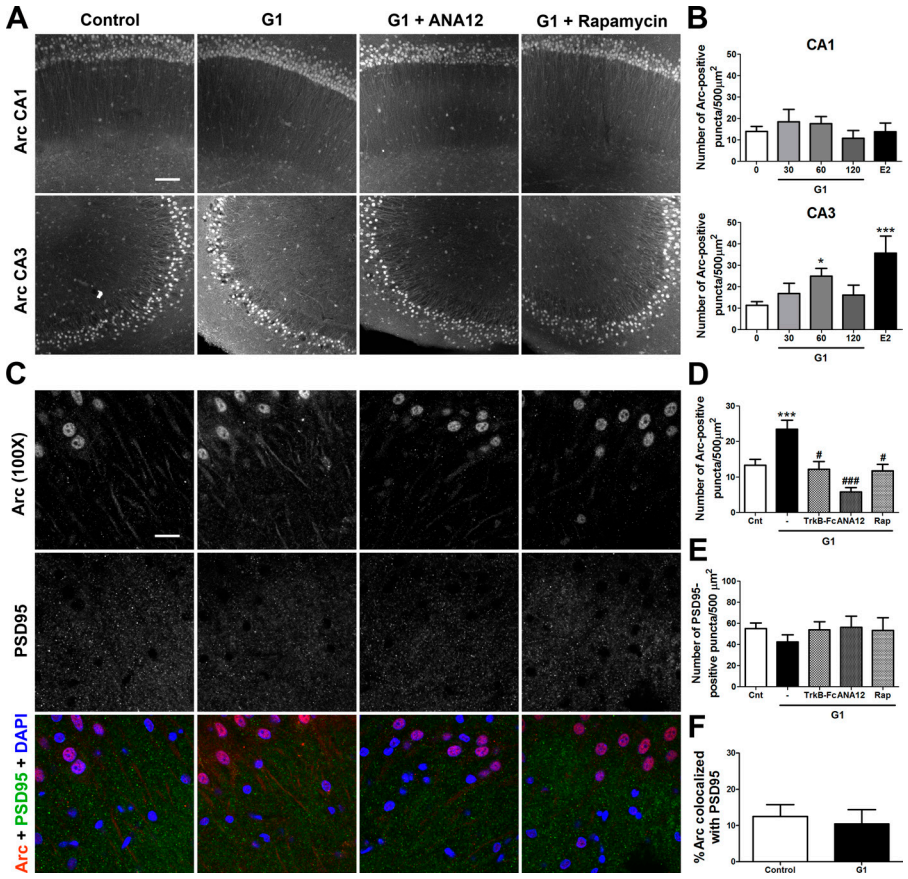

Figure 4. **G1 stimulates mTOR-dependent Arc synthesis in CA3 through BDNF release.** Hippocampal slices were pretreated with DMSO/IgG-Fc (Cnt), TrkB-Fc, ANA-12, or rapamycin, and then incubated with G1 or E_2 for an additional 60 min or the indicated times. (A) Representative images of Arc immunostaining in CA1 and CA3 under various experimental conditions. Bar, 100 µm. (B) Quantification of density of Arc-positive punctas in CA1 stratum radiatum (CA1sr) and CA3sr. *, $P < 0.05$; ***, $P < 0.001$ versus control (n = 3–16, one-way ANOVA). (C) High-magnification images of CA3 from slices double-stained for Arc (red) and PSD95 (green) along with DAPI (blue). Bar, 20 µm. (D and E) Quantification of the density of Arc (D)- and PSD95 (E)-positive punctas in CA3sr. ***, $P < 0.001$ versus control; #, $P < 0.05$; ###, $P < 0.001$ versus G1 (n = 6–29, one-way ANOVA). (F) Percentage of Arc-positive punctas that colocalized with PSD95 (M1 coefficient, n = 11–12). Error bars indicate means ± SEM.

within the nucleus), with a faint staining in dendrites (Fig. 4, A and C). Treatment of hippocampal slices with G1 or E_2 strongly increased Arc immunostaining in CA3 but not in CA1. These effects were restricted to the apical dendrites of pyramidal neurons (Fig. 4, A–C), a result consistent with the data obtained by immunoblots in P2 fractions (Fig. 3). We quantified the number of Arc-positive puncta at different time points after G1 treatment across different hippocampal subfields; a significant increase was observed in CA3 stratum radiatum (CA3sr) 1 h after G1 application, which returned to baseline by 2 h (Fig. 4 B). A similar transient increase in Arc expression has been previously described in cell lines after E_2 treatment (Kühnle et al., 2013). In contrast, neither G1 (at any of the time points tested) nor E_2 modified Arc immunostaining in CA1 (Fig. 4 B). Furthermore, G1-induced increase in Arc immunostaining in CA3 was completely blocked by the TrkB receptor antagonist ANA12, as well as by TrkB-Fc and rapamycin (Fig. 4, A, C, and D). Double staining with the postsynaptic marker PSD95 showed no significant changes in the colocalization of Arc with PSD95 after G1 treatment, as neither the percentage of Arc puncta colocalized with PSD95 (Fig. 4 F) nor the Pearson's coefficient was modified (0.092 ± 0.052 and 0.101 ± 0.05 for DMSO- and G1-treated slices, respectively; n = 11–12). PSD95 immunostaining also remained unaffected under all the experimental conditions tested; a slight decrease was found after G1 treatment, but the effect was not statistically significant (Fig. 4, C and E). Collectively, these results indicate that GPER1 activation transiently stimulates local Arc synthesis in field CA3 via BDNF release and subsequent activation of the mTOR signaling pathway.

Arc has been implicated in AMPA receptor endocytosis during synaptic plasticity (Rial Verde et al., 2006; Waung et al., 2008; Peebles et al., 2010; Liu et al., 2012) and after hormone stimulation (Chen et al., 2014). Therefore, we tested the effects of GPER1 activation on the levels of several AMPA receptor subunits in membrane and cytosolic fractions from hippocampal slices. Treatment with G1 for 1 h significantly reduced the membrane levels of GluA1, which returned to baseline by 2 h after G1 application. A concomitant increase of GluA1 in the cytosolic fraction was found 1 h after G1 stimulation, returning to basal levels 1 h later (Fig. 5 A). In contrast, the levels of GluA2/3 remained constant both in the membrane and cytosolic fractions under the same experimental conditions (Fig. 5 B). We then analyzed the expression of PSD95 in both fractions to validate the preparations used for this study. As expected, membrane fractions were enriched in PDS95, whereas PSD95 expression was barely detectable in the cytosolic fraction. No differences were observed in PSD95 levels after G1 treatment at any of the time points tested (Fig. 5 C).

Changes in GluA1 occurred in parallel to the increase in local Arc synthesis induced by G1, observed both by immunostaining (Fig. 4 B) and by immunoblotting (Fig. 3 C). Thus, we determined whether protein synthesis inhibitors could inhibit the effect of G1 on AMPA receptor endocytosis. Pretreatment with either rapamycin or cycloheximide completely blocked both the decrease in membrane GluA1 levels as well as the increase in the cytosol induced by G1 (Fig. 5, D and E). Similarly, G1-stimulated GluA1 internalization was totally suppressed by ANA12 (Fig. S2). However, we did not detect any significant changes in GluA1 levels after treat-

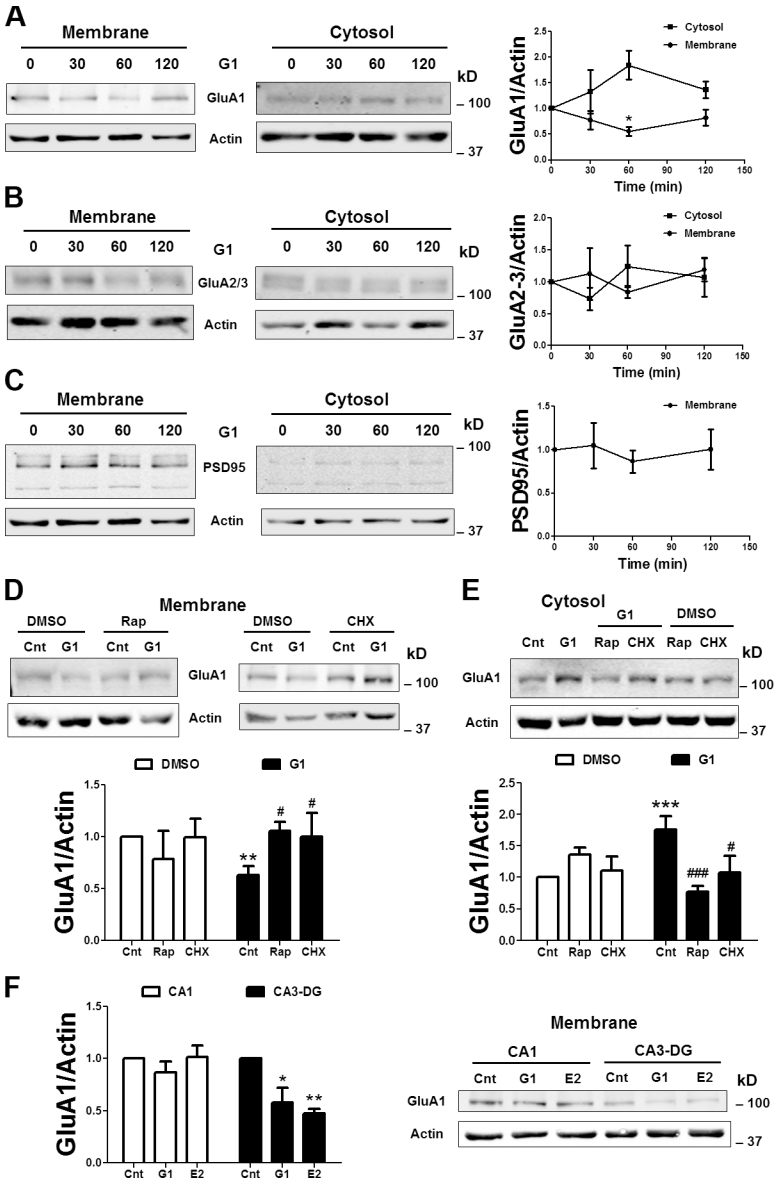

Figure 5. **G1 induces GluA1 internalization via mTOR-dependent protein synthesis.** (A–D) Whole hippocampal slices were pretreated with DMSO, cycloheximide, or rapamycin for 30 min and then incubated with G1 for an additional 60 min or the indicated times. CA1 and CA3-DG mini-slices were treated with G1 or E2 for 1 h. At the end of treatments, samples were homogenized and processed for Western blotting after membrane fractionation. Data are presented as the ratio (fold of control) of GluA1 over actin (A; n = 4–8), GluA2/3 over actin (B; n = 4–7), PSD95 over actin (C; n = 4–8), or GluA1 over actin (D–F; n = 3–11). *, $P < 0.05$; **, $P < 0.01$; ***, $P < 0.001$, as compared with control. #, $P < 0.05$; ###, $P < 0.001$, as compared with G1 alone (one- or two-way ANOVA). The actin panels in both A and C look very similar because they show the same data. Images in these two panels come from the same blot, in which different primary and secondary antibodies were used. Thus, the same actin blot serves as loading control for both GluA1 and PSD95. They have been separated in two panels for consistency in figure formatting. Error bars indicate means ± SEM.

ment with E_2, although a trend was observed in the cytosolic fraction (Fig. S2). We have previously reported that estrogen rapidly increases membrane GluA1 levels in CA1 (Zadran et al., 2009), an effect mediated by ERβ (Kramár et al., 2009). Thus, this effect could counteract the decrease in membrane GluA1 in CA3, given that we used whole hippocampal slices for these experiments. To address this issue, we used mini-slices in which the CA1 region was microdissected from the CA3-DG regions. We preserved the mossy fiber pathway, as it has been shown that modulation of spine density in CA3 by estrogen requires the input from the DG (Sato et al., 2007). Treatment with either G1 or E_2 reduced GluA1 membrane levels in CA3-DG but not in CA1 (Fig. 5 F), a result consistent with their region-specific effects on Arc synthesis (Fig. 4 B). These results seem to differ from those previously reported by our laboratory in which E_2 increased membrane GluA1 levels in CA1 mini-slices (Zadran et al., 2009). However, the different times of treatment used (60 min vs. 10 min) could account for the differences between the studies, as the acute effects of estrogen on AMPA receptor–mediated transmission are transient, lasting only up to 30 min (Kramár et al., 2009).

GPER1 activation modulates mGluR-LTD in CA3

The above results showed that G1 application stimulates the same series of events in DG-CA3 shown to be associated with mGluR-LTD at CA3-CA1 synapses, namely increased Arc translation and GluA1 internalization (Waung et al., 2008). Thus, we tested whether G1 could induce LTD in the mossy fiber pathway, the same way that DHPG does in the Schaffer collateral pathway. However, field excitatory postsynaptic potentials (fEPSPs) recorded in CA3sr with stimulation of the mossy fibers did not significantly change in response to G1 application, even when G1 was applied for up to 1 h and synaptic AMPA receptor responses were pharmacologically isolated by blocking NMDA and $GABA_A$ receptors (Fig. S3). We then determined whether G1 could modulate mGluR-LTD in CA3. Hippocampal slices were stimulated with DHPG (100 µM, 10 min) 1 h after either vehicle or G1 application (the time at which the effects on Arc and GluA1 were observed). In vehicle-pretreated slices, DHPG induced a transient depression of fEPSPs but failed to induce LTD. In marked contrast, DHPG induced robust LTD in slices pretreated with G1 (Fig. 6, A and B). These results indicate that

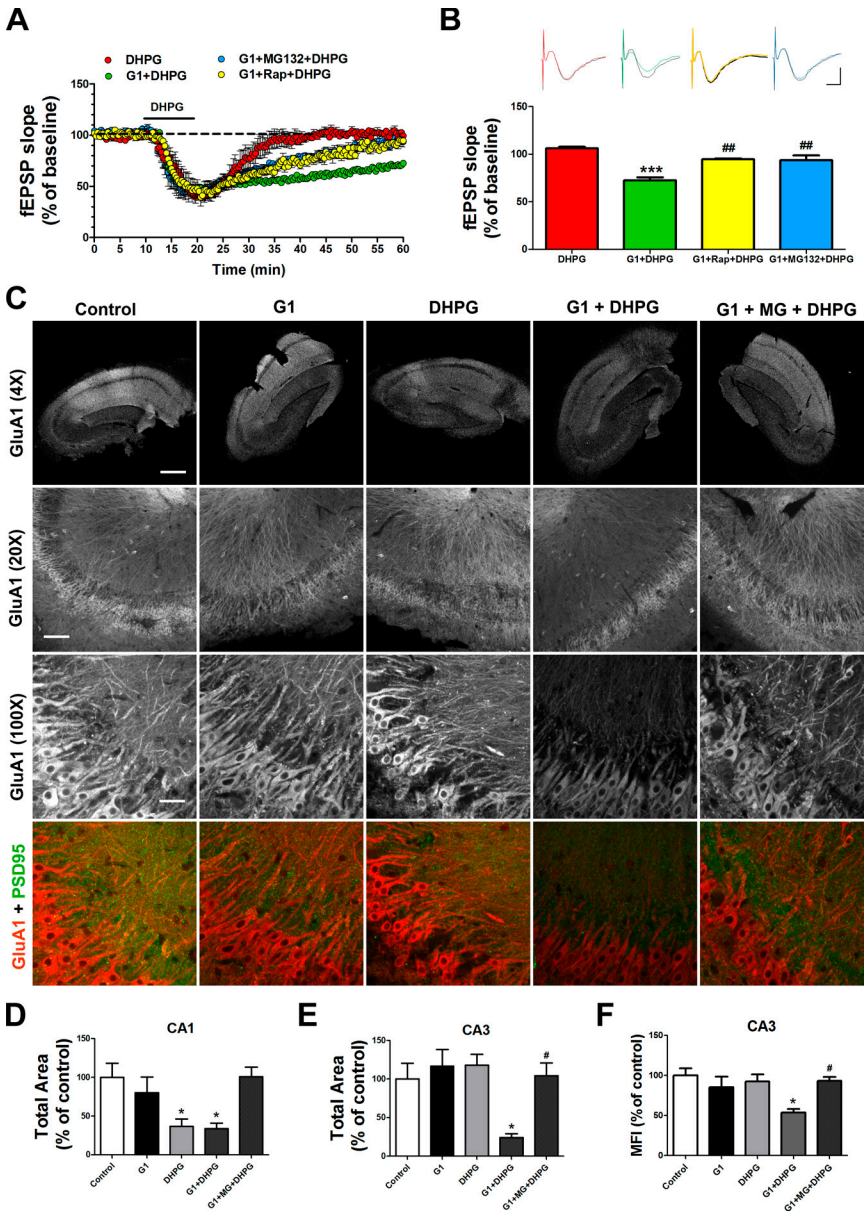

Figure 6. **GPER1 activation and proteasome activity are required for mGluR-LTD in CA3.** Hippocampal slices were incubated with DMSO or G1 for 1 h and then treated with DHPG for 15 min, unless otherwise stated. Treatment with rapamycin or MG132 was performed 20–30 min before G1 or DHPG application, respectively. (A) Rapamycin and MG132 blocked LTD induced by G1+DHPG in CA3. DHPG alone (100 µM, 10 min) did not induce LTD in CA3. (B) Traces (top) and averaged values of slopes (bottom) of fEPSPs measured in CA3 50 min after DHPG application. Bar, 0.5 mV/5 ms. ***, $P < 0.001$ versus control; ##, $P < 0.01$ versus G1+DHPG ($n = 3$, one-way ANOVA). (C) Representative images of double immunostaining for GluA1 (red) and PSD95 (green) under various experimental conditions. High-magnification images correspond to the CA3 pyramidal layer. Bars: (4×) 400 µm; (20×) 100 µm; (100×) 20 µm. (D–F) Quantification of GluA1 immunostaining by means of total area and mean fluorescence intensity (MFI) in CA1 (D) and CA3 (E and F). *, $P < 0.05$ versus control; #, $P < 0.05$ versus G1+DHPG ($n = 4–10$, one-way ANOVA). Error bars indicate means ± SEM.

DHPG can only trigger LTD in CA3 after previous stimulation of GPER1. To verify that activation of mTOR-dependent protein synthesis by G1 contributes to its effects on mGluR-LTD, we applied rapamycin 20 min before G1 treatment followed by DHPG application. LTD was abolished under these conditions (Fig. 6, A and B), indicating that mTOR activity is required for G1-mediated modulation of mGluR-LTD in CA3.

To investigate the mechanisms underlying CA3 mGluR-LTD and its modulation by G1, we compared the effects of G1+DHPG versus DHPG alone on Arc expression across different hippocampal areas. Treatment with DHPG alone did not significantly affect the number of Arc-positive puncta in CA3 (as compared with control), nor did it further enhance the effect of G1 on Arc immunostaining in this area (Fig. S1 B). Instead, DHPG increased Arc immunostaining in CA1, as previously reported (Waung et al., 2008), but the effect was not further stimulated by G1 preapplication (Fig. S1 A). These immunohistochemical data confirmed that G1 and DHPG stimulate Arc synthesis in a region-specific manner, and do not interact with each other in the regulation of local Arc expression. In addition, DHPG alone did not modify Arc levels in whole hippocampal slices, as determined by immunoblots, but it significantly increased them in the presence of G1 (Fig. S1 C). This is most likely due to additive effects of the two compounds in CA3 and CA1. These results also indicate that mGluR activation does not contribute to the increase in Arc synthesis during mGluR-LTD in CA3.

We next studied the effects of G1 and DHPG on GluA1 expression and localization in hippocampal slices by immunohistochemistry. Under control conditions, GluA1 staining using a C-terminal antibody was particularly strong in stratum radiatum and oriens of CA1, and to a smaller extent in CA3sr. High-magnification images showed clear staining in cell bodies and dendrites of CA3 pyramidal neurons, which partially colocalized with PSD95 (Fig. 6 C). Incubation of hippocampal slices with G1 for 1 h did not modify GluA1 staining in any of the regions studied. However, DHPG treatment significantly reduced GluA1 immunofluorescence in CA1 but not in CA3 (Fig. 6, C–F). These

effects are consistent with the DHPG-induced region-specific regulation of Arc synthesis shown in Fig. S1, and could account for the inability of DHPG to induce LTD in CA3, as opposed to CA1. However, a significant reduction in GluA1 staining was found in CA3 when DHPG was applied after G1 treatment (Fig. 6, C, E, and F). Notably GluA1 immunofluorescence in CA1 did not change in response to G1+DHPG treatment, as compared with DHPG alone (Fig. 6, C and D). These effects were reproduced with the use of a different antibody targeting the N-terminal region of GluA1 (Fig. S4). Overall, these results indicated that DHPG rapidly down-regulates GluA1 expression in CA3 only after previous activation of GPER1, an effect consistent with the requirement for GPER1 activation in mGluR-LTD in this area.

mGluR-LTD in CA3 is associated with GluA1 degradation by the ubiquitin–proteasome system (UPS)

The decrease in GluA1 levels in CA3 observed after G1+DHPG treatment suggested that GluA1-containing AMPA receptors might undergo rapid proteolysis in response to mGluR activation. Previous studies have reported that GluA1 is degraded by the UPS during physiological or pathological conditions (Fu et al., 2011; Yuen et al., 2012; Widagdo et al., 2015). We thus determined whether UPS inhibition could affect GluA1 down-regulation during mGluR-LTD. Treatment of hippocampal slices with MG132 (25 µM) 30 min before DHPG application completely blocked the reduction in GluA1 immunostaining in CA1 and CA3 induced by G1+DHPG (Fig. 6, C–F). These results were also replicated using an N-terminal GluA1 antibody by immunohistochemistry (Fig. S4) and immunoblotting in whole hippocampal slices (Fig. S5 A). Treatment with MG132 alone did not affect GluA1 levels (Fig. S5 A), suggesting that GluA1 is not degraded by UPS under basal conditions.

The phosphorylation state of GluA1 at specific serine residues regulates AMPA receptor internalization and has been implicated in LTD (Lee et al., 2000; Gladding et al., 2009). We determined the effects of proteasome inhibition on GluA1 phosphorylation during mGluR-LTD in whole hippocampal slices. Treatment with G1+DHPG increased GluA1 phosphorylation at Ser845 and the effect was blocked by MG132 (Fig. S5 B). In contrast, phosphorylation of GluA1 at Ser831 was not affected under any of the conditions tested (Fig. S5 C). These results indicated that mGluR-LTD was associated with phosphorylation of GluA1 at Ser845.

Previous studies have found that proteasome inhibition blocked mGluR-LTD in CA1 (Hou et al., 2006; Bernard et al., 2014), although opposite effects have also been reported (Citri et al., 2009). To evaluate the contribution of UPS activity to mGluR-LTD in CA3, we applied MG132 30 min before DHPG treatment (i.e., 30 min after G1). Under these conditions, LTD induced by G1+DHPG was significantly impaired (Fig. 6, A and B), indicating that proteasome activity is required for mGluR-LTD in this region.

Arc protein has also been identified as a UPS target (Greer et al., 2010). Thus, the inhibitory effects of MG132 on mGluR-LTD could also be due to changes in Arc protein levels. However, treatment with MG132 did not modify the increase in Arc levels induced by G1+DHPG in whole hippocampal slices. MG132 alone increased Arc levels but the effect was not statistically significant (Fig. S1 D).

Changes in free ubiquitin levels have been associated with fluctuations in UPS activity (Lee et al., 2010; Santos et al., 2015). To further investigate the role of UPS in mGluR-LTD, we determined free ubiquitin levels in whole hippocampal slices at different time points after DHPG application. DHPG treatment caused a significant decrease in free ubiquitin levels at 15 min, which then gradually returned to baseline (Fig. 7 A). These effects were still present in the presence of MG132, indicating that changes in free ubiquitin levels induced by DHPG were independent of proteasome activity or occur upstream of UPS. These results also suggested that DHPG rapidly and transiently stimulated protein polyubiquitination. To verify this hypothesis, we treated hippocampal slices with DMSO or G1+DHPG in the presence of MG132 (to prevent degradation of ubiquitinated proteins), and samples were probed with an anti-ubiquitin antibody, which recognizes both mono- and polyubiquitinated proteins. A marked increase in the levels of ubiquitinated proteins was found after treatment with G1+DHPG, as compared with control samples (Fig. 7 B). The effects were particularly evident for high molecular weight proteins, suggesting that mGluR-LTD is associated with protein polyubiquitination rather than monoubiquitination. To determine whether GluA1 was ubiquitinated under the same experimental conditions, homogenates from whole hippocampal slices were immunoprecipitated with a GluA1 antibody and precipitated proteins were immunoblotted using the anti-ubiquitin antibody. Increased ubiquitination was found after GluA1 immunoprecipitation in samples treated with G1+DHPG, as compared with control (Fig. 7 B). Immunoblot analysis using a GluA1 antibody confirmed that the observed high molecular weight band corresponded to GluA1 (Fig. 7 B). In contrast, no ubiquitination or GluA1 immunoreactivity was detected under any experimental condition in samples immunoprecipitated with IgG-coated agarose beads (Fig. 7 B). These results strongly suggest that GluA1 undergoes UPS-mediated degradation during mGluR-LTD. However, we cannot rule out that other GluA1-associated proteins are also ubiquitinated during mGluR-LTD, as the immunoprecipitation experiments were conducted under nonreducing conditions.

Discussion

Different forms of mGluR-dependent LTD in the hippocampus

LTD triggered by activation of type-I mGluR in CA1 represents the most studied form of mGluR-LTD in hippocampus, but the underlying mechanisms are still under debate. It is now widely accepted that DHPG-induced LTD in CA1 requires local protein synthesis, and in particular Arc translation (Waung et al., 2008). However, the nature of the signaling pathways and translation factors involved remains controversial. Studies by different groups have identified the Akt–mTOR signaling pathway as a major mediator of mGluR-LTD, while the role of ERK is less clear (Gallagher et al., 2004; Hou and Klann, 2004; Bernard et al., 2014). Our results indicate that GPER1-mediated Arc synthesis and GluA1 internalization in CA3 requires stimulation of mTOR-dependent protein translation, as the effects were blocked by rapamycin and cycloheximide. However, these events were necessary but not sufficient to trigger LTD in this hippocampal area, which might be also the case for DHPG-induced LTD in CA1, as recently proposed (Bernard et al., 2014). In addition, incubation with DHPG alone did not increase Arc synthesis or modify GluA1 levels in CA3, whereas it did in CA1; only when applied after GPER1 activation did DHPG re-

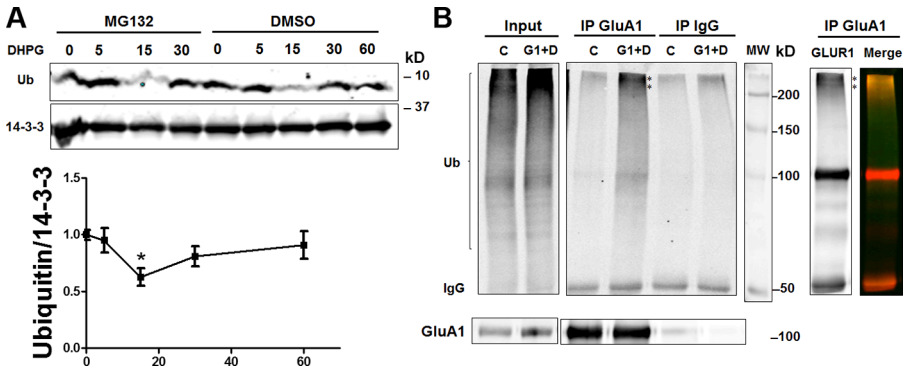

Figure 7. **DHPG stimulates proteasome activity and GluA1 ubiquitination.** (A) Hippocampal slices were treated with DHPG in the absence or presence of MG132 for the indicated times and samples were homogenized and processed for Western blotting in 16% tricine gel. Data are presented as the ratio (fold of control) of free ubiquitin (Ub) over 14-3-3γ. *, $P < 0.05$ versus control (n = 7–10, one-way ANOVA). Error bars indicate means ± SEM. (B) Hippocampal slices were incubated with DMSO or G1+DHPG (G1+D) in the presence of MG132. Samples were then analyzed by Western blotting before (input) or after immunoprecipitation (IP) with GluA1 antibody or IgG. The right panel shows an immunoblot for GluA1 and a merged image of immunoblots for GluA1 (red) and ubiquitin (green). Asterisks indicate bands corresponding to ubiquitinated GluA1.

duce GluA1 immunostaining and induce LTD in CA3. Further studies are needed to mechanistically understand why DHPG alone is unable to stimulate Arc synthesis and hence to induce LTD in this hippocampal area.

While G1 application induced GluA1 internalization, it did not modify baseline fEPSP or synaptic AMPA receptor–mediated responses. A possible explanation for this paradox could be that G1 mostly affects internalization of extrasynaptic AMPA receptors, which do not contribute to synaptic responses. This assumption is supported by our finding that Arc and PSD95 colocalization was not altered by G1 treatment. However, this effect might become critical after DHPG-induced activation of UPS-induced degradation of these receptors, thus resulting in a decrease of GluA1-containing AMPA receptors and in LTD.

Role of the UPS in mGluR-LTD

The results presented here strongly suggest that DHPG-induced activation of the UPS is the rate-limiting step that triggers the long-lasting changes in AMPA receptor–mediated synaptic transmission necessary to produce LTD. MG132 prevented G1+DHPG–induced GluA1 down-regulation and LTD in CA3, indicating that UPS activity is required for mGluR-LTD in this hippocampal area, a result consistent with previous findings in CA1 (Hou et al., 2006; Bernard et al., 2014). Furthermore, our data indicated that treatment with G1+DHPG increased GluA1 polyubiquitination in hippocampal slices. Although GluA1 has been previously reported to be ubiquitinated during synaptic plasticity or after repeated stress (Fu et al., 2011; Yuen et al., 2012; Widagdo et al., 2015), an association between UPS-mediated GluA1 degradation and mGluR-LTD has not yet been described. Nevertheless, degradation of fragile X mental retardation protein could also contribute to the regulation of mGluR-LTD by the UPS, as previously proposed (Hou et al., 2006).

The time course for DHPG-induced reduction of free ubiquitin levels is consistent with the effects of G1+DHPG on GluA1 immunostaining and ubiquitination, which were also observed 15 min after DHPG treatment. Decrease in free ubiquitin levels could result from inhibition of UPS activity (Santos et al., 2015) or from inhibition of deubiquitinating enzymes (Lee et al., 2010). Our data indicated that DHPG stimulated GluA1 polyubiquitination (and possibly of other proteins), which could produce a transient decrease in free ubiquitin and stimulation of UPS activity. However, whether this occurs through activation of ubiquitin ligases or by inhibition of deubiquitinating enzymes remains to be addressed.

Dephosphorylation of GluA1-containing AMPA receptors at Ser845 has been suggested to drive AMPA receptor endocytosis during NMDA receptor–mediated LTD (NMDA-LTD), whereas no changes in Ser845 were found after mGluR-LTD in CA1 (Lee et al., 2000; Gladding et al., 2009; He et al., 2009). In the present study, we found that G1+DHPG increased the phosphorylation of GluA1 at Ser845 but not at Ser831, further indicating the existence of differences between mGluR-LTD in CA1 and CA3. Although only a very small fraction of GluA1 seem to be phosphorylated at Ser845 according to a recent study (Hosokawa et al., 2015), phosphorylation at this residue has been shown to be important for the stabilization of GluA1 homomers at perisynaptic sites (He et al., 2009). Furthermore, the effects of G1+DHPG on Ser845 were prevented by MG132, a result in agreement with studies showing that proteasome inhibitors block AMPA receptor endocytosis (Colledge et al., 2003; Patrick et al., 2003). These effects seem to be in conflict with recent findings showing that AMPA receptor ubiquitination is not required for receptor internalization (Widagdo et al., 2015). Nevertheless, the effects of proteasome inhibition on GluA1 dephosphorylation/internalization could rely on changes in other proteins involved in AMPA receptor trafficking, such as PSD95 (Colledge et al., 2003). In any event, our results are also consistent with the notion that GluA1 internalization precedes receptor ubiquitination, and moreover they indicate that these events are regulated by different receptors (GPER1 and mGluR, respectively) in CA3.

Mechanisms for estrogen modulation of LTD and memory consolidation

E_2 has been previously shown to enhance mGluR-LTD in CA1 through activation of classical ERs (Shiroma et al., 2005). Consistent with these findings, G1 was unable to induce Arc synthesis or GluA1 internalization in this area, and hence it is unlikely that GPER1 is involved in these effects. Although the mechanisms underlying estrogen modulation of mGluR-LTD in CA1 have not yet been explored, they could be due to the direct association of ERα/β with mGluA1 (Boulware et al., 2013). In summary, mGluR-LTD in CA1 and CA3 appears to be regulated by different types of ERs, and, in particular, while E_2 potentiates the effects of DHPG on LTD in CA1, it gates

mGluR-LTD in CA3, providing a novel mode of regulation of synaptic plasticity by estrogen.

Activation of both ERα/β and GPER1 by E_2 rapidly improves memory consolidation in a variety of learning paradigms when E_2 is administered immediately after acquisition (Ervin et al., 2013). Similarly, chronic or short-term activation of GPER1 has been reported to enhance spatial memory in ovariectomized rats (Hammond et al., 2009; Hawley et al., 2014), whereas chronic treatment with a GPER1 antagonist impairs spatial memory acquisition both in intact and ovariectomized rats (Hammond et al., 2012). Furthermore, E_2 injections into the dorsal hippocampus increase mTOR phosphorylation, an effect required for increase in memory consolidation (Fortress et al., 2013). Collectively, these studies highlight the importance of GPER1 and of the Akt/mTOR signaling pathway in estrogen modulation of learning and memory. In addition, mossy fiber LTD has been implicated in spatial memory (Hagena and Manahan-Vaughan, 2011), suggesting that the mechanism described here could play an important role in estrogen-induced cognitive enhancement. Because most behavioral studies with estrogen have been performed in ovariectomized rats, it would be important to study whether a similar modulation of mGluR-LTD by estrogen occurs in cycling females. Likewise, more studies are also needed to understand how brain-derived estrogen regulates male cognition, considering that the levels of estrogen in male hippocampus are higher than those in female rats at any stage of the estrous cycle (Hojo et al., 2011). In this regard, activity-dependent changes in locally synthesized estrogen could be involved in the rapid modulation of synaptic plasticity by estrogen in adult male rats (Hojo et al., 2004).

Roles of GPER1 and BDNF in mossy fiber synaptic plasticity

Our previous studies have identified a novel signaling pathway by which BDNF regulates dendritic protein synthesis, which involves calpain-mediated PTEN degradation upstream of Akt and mTOR activation (Briz et al., 2013). We also found that estrogen stimulates the same signaling cascade in hippocampal slices via activation of GPER1 (Briz and Baudry, 2014). Here, we report that E_2- and G1-induced increase in Akt/mTOR signaling and protein translation requires BDNF release and TrkB receptor activation. Our results are in good agreement with a previous report showing that estrogen stimulates BDNF release from dentate granule cells, which in turn enhances PSD95 expression and synaptogenesis in CA3 (Sato et al., 2007), although the effects were examined at a later time point (24 h after estrogen treatment). We did not observe significant changes in PSD95 immunostaining 1 h after G1 treatment, suggesting that the estrogenic effects on PSD95 expression may involve a genomic mechanism. Supporting this notion, a recent in vivo study reported that PSD95 expression increased in CA3 6 h after G1 administration (Waters et al., 2015).

GPER1 activation has been reported to regulate the release of growth factors and hormones, as well as neurotransmitters (Filardo et al., 2000; Mårtensson et al., 2009; Hammond et al., 2011). We now show that both E_2 and G1 rapidly (within 1 h) stimulate BDNF release from cultured neurons and regulate synaptic plasticity in CA3 through a rapid nongenomic mechanism. Consistent with our results, Sato et al. (2007) showed that estrogen-induced BDNF release was not blocked by the ER antagonist ICI182780 but involves instead PKA activity, which is known to be downstream of GPER1 activation (Filardo et al., 2002; Hsieh et al., 2007; Zucchetti et al., 2014). PKA activation also stimulates BDNF release during different forms of synaptic plasticity (Patterson et al., 2001; Taniguchi et al., 2006), including at mossy fiber–CA3 synapses (Sivakumaran et al., 2009). GPER1 has been recently detected in hippocampal dendritic spines and axon terminals (Akama et al., 2013; Waters et al., 2015), being particularly abundant in the CA3 stratum lucidum (Waters et al., 2015). Notably, this particular CA3 subfield is where the axons of the dentate granule cells make synaptic contacts with CA3 pyramidal neurons, and where BDNF-containing presynaptic boutons are located (Danzer and McNamara, 2004; Scharfman and MacLusky, 2014), further supporting the role of GPER1 in BDNF release. In addition, aromatase expression has been detected in terminal processes in CA3 (Hojo et al., 2004), further suggesting that locally synthesized estrogen may regulate synaptic plasticity in this hippocampal area.

Emerging evidence indicates that BDNF is an important mediator of steroid modulation of mossy fiber synaptic plasticity and sprouting (Scharfman and MacLusky, 2014). For instance, Scharfman et al. (2003) found an increase in BDNF immunoreactivity and synaptic excitability in CA3 pyramidal neurons at proestrous in female rats, the later effect being reversed by the TrkB receptor antagonist K252a. Despite the overall low expression of BDNF in hippocampus of male rats, as compared with females (Scharfman et al., 2003), BDNF protein has been reported to rapidly increase after acute slice preparation, especially in the CA3 pyramidal cell layer (Danzer et al., 2004). In our study, BDNF-mediated modulation of Arc synthesis and GluA1 levels was restricted to CA3. Collectively, these findings support the idea that BDNF plays a prominent role in mossy fiber plasticity.

Concluding remarks

The mechanism underlying GPER1-mediated regulation of mGluR-LTD we identified represents a new type of estrogen-mediated modulation of synaptic plasticity. In contrast to the effects of estrogen on LTP in CA1, where estrogen lowers the threshold and enhances the magnitude of LTP consolidation (Kramár et al., 2009), the estrogen effect in CA3 appears to "prime" synapses to undergo LTD if the appropriate stimulation occurs. In the absence of such stimulation, changes in synaptic proteins (i.e., Arc and GluA1) elicited by GPER1 activation return to basal conditions. This phenomenon fits well with the two-step wiring plasticity model proposed for estrogen modulation of NMDA receptor–mediated synaptic plasticity (Srivastava et al., 2008). In that case, estrogen rapidly and transiently down-regulates GluA1 (with a similar time-course as the one we found here) to generate silent synapses, which undergo potentiation if NMDA stimulation occurs within the appropriate interval of time. Intriguingly, our study and others indicate that estrogen enhances mGluR-LTD, whereas it transforms NMDA-LTD into LTP (Shiroma et al., 2005), an effect apparently mediated by different ER isoforms (Mukai et al., 2007). Therefore, the type of stimulation as well as the nature of the activated estrogen receptor would modify synaptic responses toward potentiation or depression, which provide a large repertoire for estrogen-mediated modulation of synaptic plasticity.

Materials and methods

Animals were treated in accordance with the principles and procedures of the National Institutes of Health Guide for the Care and Use of Laboratory Animals; all protocols were approved by the Institutional Animal Care and Use Committee of Western University of Health Sciences.

Acute hippocampal slice preparation

Hippocampal slices were prepared from 2–4-mo-old male Sprague-Dawley rats, as described previously (Briz and Baudry, 2014), with minor modifications. In brief, isolated hippocampi were transferred to oxygenated, ice-cold cutting medium containing (in mM): sucrose (220), NaCl (20), $NaHCO_3$ (26), D-glucose (10), KCl (2.5), NaH_2PO_4 (1.25), and $MgSO_4$ (2), and cut into 350-µm-thick transverse slices. Hippocampal slices were maintained in a recovery chamber with artificial cerebrospinal fluid (aCSF) medium, containing (in mM): NaCl (124), KCl (2.5), $CaCl_2$ (2.5), $MgSO_4$ (1.5), NaH_2PO_4 (1.25), $NaHCO_3$ (24), and D-glucose (10), and saturated with 95% O_2/5% CO_2, for 1 h at 37°C. Hippocampal slices were then transferred into screw-cap microfuge tubes containing freshly oxygenated aCSF medium in the presence of various drugs. CA1 and CA3-DG mini-slices were obtained by dissecting out the respective regions under a light microscope, before transferring them into microfuge tubes.

Drug treatments

Slices were incubated with 10 nM E_2 (EMD Millipore) or 100 nM G1 (Tocris Bioscience) at 37°C for the indicated periods of time. Alternatively, slices were incubated with 100 nM PPT (Tocris Bioscience) or 10 nM DPN (Tocris Bioscience) for 1 h. Treatment with DHPG (100 µM; Tocris Bioscience) was generally performed 1 h after G1 application and lasted 15 min, unless stated otherwise. In some experiments, slices were pretreated for 30 min with different inhibitors or antagonists, including ANA-12 (50 µM; Tocris Bioscience), cycloheximide (25 µM; Tocris Bioscience), MG132 (25 µM; EMD Millipore), rapamycin (1 µM; Cell Signaling Technology), and G36 (1 µM; Azano Biotech). TrkB-Fc (2 µg/ml; R&D Systems) or IgG-Fc (2 µg/ml; Bethyl Laboratories, Inc.) were preincubated for 1 h before chemical treatment.

Electrophysiology

After 2 h of incubation in the recording chamber, a single glass pipette filled with 2 M NaCl was used to record fEPSPs elicited by chemical stimulation (bath application of 100 µM DHPG). Responses in CA3sr were recorded through a differential amplifier (DAM 50; World Precision Instruments, Inc.) with a 10 kHz high-pass and 0.1 Hz low-pass filter. Data were collected and digitized by Clampex (Molecular Devices), and the slope of fEPSP was analyzed. The LTD level was normalized to the 10-min baseline.

Membrane fractionation

Subcellular fractionation was performed as described previously (Sun et al., 2015), with minor modifications. After treatment, 4–5 hippocampal slices (or 9–10 CA1/CA3-DG mini-slices) were pooled and homogenized in ice-cold Hepes-buffered sucrose solution (0.32 M sucrose and 4 mM Hepes, pH 7.4) containing protease and phosphatase inhibitor cocktails (Thermo Fisher Scientific), 2 mM EDTA, and 2 mM EGTA. Homogenates were centrifuged at 900 *g* for 10 min to remove large debris (P1). The supernatant (S1) was then centrifuged at 11,000 *g* for 20 min to obtain the crude synaptosomal (P2) and cytosolic (S2) fractions. The P2 pellets were sonicated in RIPA buffer (Thermo Fisher Scientific) containing protease/phosphatase inhibitors. For whole homogenates, hippocampal slices were individually homogenized in RIPA buffer containing protease/phosphatase inhibitors. Protein concentrations were determined with a BCA protein assay kit (Thermo Fisher Scientific).

BDNF release assay

Detection of BDNF released into the extracellular media was performed in primary cultures of cortical neurons from embryonic day 16–18 rat pups, as described previously (Jourdi et al., 2009). In brief, primary cultures of rat cortical neurons at day in vitro 14 were first washed with warm HBSS and then incubated with TrkB-Fc (1 h, 2 µg/ml) before being treated with different estrogen receptor agonists for 1 h. At the end of treatments, medium from three to four dishes was collected and concentrated (30–40×) using filter-centrifugation through a Vivaspin 20 column (Vivascience) at 4°C. Samples were processed for immunoblotting using antibodies against BDNF (1:500, AB1779SP; EMD Millipore; 1:200, sc-546) and TrkB (1:1,000; Cell Signaling Technology).

Immunohistochemistry

Immunostaining and image acquisition were performed as described previously (Briz et al., 2015), with minor modifications. In brief, hippocampal slices were fixed in 4% paraformaldehyde for 1 h and cryoprotected in 30% sucrose for 1 h at 4°C, and sectioned on a freezing microtome at 30 µm. Sections were blocked in 0.1 M PBS containing 10% goat serum and 0.4% Triton X-100, and then incubated overnight at 4°C in 0.1 M PBS containing 5% goat serum and 0.4% Triton X-100 and the following primary antibodies: rabbit anti-Arc (1:50, sc-15325, Santa Cruz Biotechnology, Inc.; 1:500, EMD Millipore), rabbit anti-GluA1 (1:400, AB1504; EMD Millipore), mouse anti-GluA1 (1:50, sc-13152; Santa Cruz Biotechnology, Inc.), rabbit anti-PSD95 (1:50, ab18258; Abcam), and mouse anti-PSD95 (1:500, MA1-045/046; Thermo Fisher Scientific). Sections were then incubated with Alexa Fluor 594 goat anti–rabbit IgG (A-11037; Life Technologies) and Alexa Fluor 488 goat anti–mouse IgG (A-11001) for 2 h at room temperature, and sealed in slides with mounting medium containing DAPI (Vector Laboratories). Immunostained slices were examined under a confocal fluorescence microscope (Eclipse TE2000 C1; Nikon) at room temperature using EZ-C1 software. Quantification of dendritic punctas was performed using ImageJ software by counting the number of particles (2–100 pixels) per field (100× objective lens using 150 µm of pinhole aperture and 512 × 512 pixels of resolution). Colocalization analysis was performed using "Just another Colocalisation plugin" under ImageJ software and results expressed as normalized ratios of Arc-positive punctas colocalized with PSD95-positive punctas over total PSD95-positive punctas (M1 coefficient).

Immunoprecipitation

Equal amounts (2 mg) of lysate proteins were collected from hippocampal slices treated with DMSO or G1+DHPG in the presence of MG132. Samples were immunoprecipitated with protein A/G agarose beads (Thermo Fisher Scientific) previously coated with 4 µg of either GluA1 antibody (AB1504) or IgG (sc-2027). Anti-ubiquitin (Fk2; Enzo Life Sciences) and anti-GluA1 (AB1504 and sc-13152) antibodies were used for immunoblotting.

Immunoblot

After sample processing, 10–40 µg of denatured proteins were subjected to 8–15% SDS-PAGE, as described previously (Briz and Baudry, 2014). To detect free ubiquitin, samples were run in 16% tricine gels, as described previously (Schägger, 2006). The following primary antibodies were used at 1:1,000 dilution, unless otherwise stated: phospho-mTOR (Ser2448) and mTOR (both from Cell Signaling Technology), phospho-Akt (Ser473) and Akt (both from Cell Signaling Technology), PTEN (Cell Signaling Technology), αCaMKII

(Cell Signaling Technology), ubiquitin (Cell Signaling Technology), phospho-GluA1 (Ser831; EMD Millipore), phospho-GluA1 (Ser845; EMD Millipore), GluA1 (EMD Millipore), GluA1 (1:50, sc-13152), GluA2/3 (1:500; EMD Millipore), PSD95 (1:2,000; Thermo Fisher Scientific), Arc (1:200, sc-15325), 14-3-3γ (1:500, sc-1019), and actin (1:10,000; EMD Millipore).

Statistical analysis

Statistical comparisons were made by using one-way analyses of variance (ANOVA) followed by Dunnett's multiple comparison test and two-way ANOVA followed by Bonferroni posttest analysis. Results were generally calculated as means ± SEM from the indicated number of independent experiments and expressed as fold of the indicated control. P-values >0.05 were regarded as not significant.

Online supplemental material

Fig. S1 shows region-specific effects of G1 and DHPG on Arc immunostaining. Fig. S2 shows that G1-induced GluA1 internalization requires TrkB receptor activation. Fig. S3 shows the effects of G1 on baseline fEPSPs in the CA3 area of the hippocampus. Fig. S4 shows that MG132 blocks down-regulation of GluA1 immunostaining by G1+DHPG. Fig. S5 shows the effects of MG132 and G1+DHPG on GluA1 phosphorylation. Online supplemental material is available at http://www.jcb.org/cgi/content/full/jcb.201504092/DC1. Additional data are available in the JCB DataViewer at http://dx.doi.org/10.1083/jcb.201504092.dv.

Acknowledgments

We thank Dr. Steve Standley and Mariam Avetisyam for their assistance with neuronal cultures.

This work was supported by grant P01NS045260-01 from the National Institute of Neurological Disorders and Stroke (PI: Dr. C.M. Gall).

The authors declare no competing financial interests.

Submitted: 21 April 2015
Accepted: 19 August 2015

References

Aakalu, G., W.B. Smith, N. Nguyen, C. Jiang, and E.M. Schuman. 2001. Dynamic visualization of local protein synthesis in hippocampal neurons. *Neuron.* 30:489–502. http://dx.doi.org/10.1016/S0896-6273(01)00295-1

Akama, K.T., L.I. Thompson, T.A. Milner, and B.S. McEwen. 2013. Post-synaptic density-95 (PSD-95) binding capacity of G-protein-coupled receptor 30 (GPR30), an estrogen receptor that can be identified in hippocampal dendritic spines. *J. Biol. Chem.* 288:6438–6450. http://dx.doi.org/10.1074/jbc.M112.412478

Bernard, P.B., A.M. Castano, K.U. Bayer, and T.A. Benke. 2014. Necessary, but not sufficient: insights into the mechanisms of mGluR mediated long-term depression from a rat model of early life seizures. *Neuropharmacology.* 84:1–12. http://dx.doi.org/10.1016/j.neuropharm.2014.04.011

Boulware, M.I., J.D. Heisler, and K.M. Frick. 2013. The memory-enhancing effects of hippocampal estrogen receptor activation involve metabotropic glutamate receptor signaling. *J. Neurosci.* 33:15184–15194. http://dx.doi.org/10.1523/JNEUROSCI.1716-13.2013

Brailoiu, E., S.L. Dun, G.C. Brailoiu, K. Mizuo, L.A. Sklar, T.I. Oprea, E.R. Prossnitz, and N.J. Dun. 2007. Distribution and characterization of estrogen receptor G protein-coupled receptor 30 in the rat central nervous system. *J. Endocrinol.* 193:311–321. http://dx.doi.org/10.1677/JOE-07-0017

Briz, V., and M. Baudry. 2014. Estrogen regulates protein synthesis and actin polymerization in hippocampal neurons through different molecular mechanisms. *Front. Endocrinol. (Lausanne).* 5:22.

Briz, V., Y.T. Hsu, Y. Li, E. Lee, X. Bi, and M. Baudry. 2013. Calpain-2-mediated PTEN degradation contributes to BDNF-induced stimulation of dendritic protein synthesis. *J. Neurosci.* 33:4317–4328. http://dx.doi.org/10.1523/JNEUROSCI.4907-12.2013

Briz, V., G. Zhu, Y. Wang, Y. Liu, M. Avetisyan, X. Bi, and M. Baudry. 2015. Activity-dependent rapid local RhoA synthesis is required for hippocampal synaptic plasticity. *J. Neurosci.* 35:2269–2282. http://dx.doi.org/10.1523/JNEUROSCI.2302-14.2015

Cazorla, M., J. Prémont, A. Mann, N. Girard, C. Kellendonk, and D. Rognan. 2011. Identification of a low-molecular weight TrkB antagonist with anxiolytic and antidepressant activity in mice. *J. Clin. Invest.* 121:1846–1857. http://dx.doi.org/10.1172/JCI43992

Chamniansawat, S., and S. Chongthammakun. 2009. Estrogen stimulates activity-regulated cytoskeleton associated protein (Arc) expression via the MAPK- and PI-3K-dependent pathways in SH-SY5Y cells. *Neurosci. Lett.* 452:130–135. http://dx.doi.org/10.1016/j.neulet.2009.01.010

Chen, T.J., D.C. Wang, H.S. Hung, and H.F. Ho. 2014. Insulin can induce the expression of a memory-related synaptic protein through facilitating AMPA receptor endocytosis in rat cortical neurons. *Cell. Mol. Life Sci.* 71:4069–4080. http://dx.doi.org/10.1007/s00018-014-1620-5

Citri, A., G. Soler-Llavina, S. Bhattacharyya, and R.C. Malenka. 2009. *N*-methyl-D-aspartate receptor- and metabotropic glutamate receptor-dependent long-term depression are differentially regulated by the ubiquitin-proteasome system. *Eur. J. Neurosci.* 30:1443–1450. http://dx.doi.org/10.1111/j.1460-9568.2009.06950.x

Colledge, M., E.M. Snyder, R.A. Crozier, J.A. Soderling, Y. Jin, L.K. Langeberg, H. Lu, M.F. Bear, and J.D. Scott. 2003. Ubiquitination regulates PSD-95 degradation and AMPA receptor surface expression. *Neuron.* 40:595–607. http://dx.doi.org/10.1016/S0896-6273(03)00687-1

Danzer, S.C., and J.O. McNamara. 2004. Localization of brain-derived neurotrophic factor to distinct terminals of mossy fiber axons implies regulation of both excitation and feedforward inhibition of CA3 pyramidal cells. *J. Neurosci.* 24:11346–11355. http://dx.doi.org/10.1523/JNEUROSCI.3846-04.2004

Danzer, S.C., E. Pan, S. Nef, L.F. Parada, and J.O. McNamara. 2004. Altered regulation of brain-derived neurotrophic factor protein in hippocampus following slice preparation. *Neuroscience.* 126:859–869. http://dx.doi.org/10.1016/j.neuroscience.2004.03.025

Dennis, M.K., A.S. Field, R. Burai, C. Ramesh, W.K. Petrie, C.G. Bologa, T.I. Oprea, Y. Yamaguchi, S. Hayashi, L.A. Sklar, et al. 2011. Identification of a GPER/GPR30 antagonist with improved estrogen receptor counterselectivity. *J. Steroid Biochem. Mol. Biol.* 127:358–366. http://dx.doi.org/10.1016/j.jsbmb.2011.07.002

Ervin, K.S., A. Phan, C.S. Gabor, and E. Choleris. 2013. Rapid oestrogenic regulation of social and nonsocial learning. *J. Neuroendocrinol.* 25:1116–1132. http://dx.doi.org/10.1111/jne.12079

Fester, L., and G.M. Rune. 2015. Sexual neurosteroids and synaptic plasticity in the hippocampus. *Brain Res.* 1621:162–169. http://dx.doi.org/10.1016/j.brainres.2014.10.033

Filardo, E.J., J.A. Quinn, K.I. Bland, and A.R. Frackelton Jr. 2000. Estrogen-induced activation of Erk-1 and Erk-2 requires the G protein-coupled receptor homolog, GPR30, and occurs via trans-activation of the epidermal growth factor receptor through release of HB-EGF. *Mol. Endocrinol.* 14:1649–1660. http://dx.doi.org/10.1210/mend.14.10.0532

Filardo, E.J., J.A. Quinn, A.R. Frackelton Jr., and K.I. Bland. 2002. Estrogen action via the G protein-coupled receptor, GPR30: stimulation of adenylyl cyclase and cAMP-mediated attenuation of the epidermal growth factor receptor-to-MAPK signaling axis. *Mol. Endocrinol.* 16:70–84. http://dx.doi.org/10.1210/mend.16.1.0758

Fortress, A.M., L. Fan, P.T. Orr, Z. Zhao, and K.M. Frick. 2013. Estradiol-induced object recognition memory consolidation is dependent on activation of mTOR signaling in the dorsal hippocampus. *Learn. Mem.* 20:147–155. http://dx.doi.org/10.1101/lm.026732.112

Fu, A.K., K.W. Hung, W.Y. Fu, C. Shen, Y. Chen, J. Xia, K.O. Lai, and N.Y. Ip. 2011. APC(Cdh1) mediates EphA4-dependent downregulation of AMPA receptors in homeostatic plasticity. *Nat. Neurosci.* 14:181–189. http://dx.doi.org/10.1038/nn.2715

Gallagher, S.M., C.A. Daly, M.F. Bear, and K.M. Huber. 2004. Extracellular signal-regulated protein kinase activation is required for metabotropic glutamate receptor-dependent long-term depression in hippocampal area CA1. *J. Neurosci.* 24:4859–4864. http://dx.doi.org/10.1523/JNEUROSCI.5407-03.2004

Gingerich, S., G.L. Kim, J.A. Chalmers, M.M. Koletar, X. Wang, Y. Wang, and D.D. Belsham. 2010. Estrogen receptor α and G-protein coupled receptor 30 mediate the neuroprotective effects of 17β-estradiol in novel murine hippocampal cell models. *Neuroscience.* 170:54–66. http://dx.doi.org/10.1016/j.neuroscience.2010.06.076

Gladding, C.M., V.J. Collett, Z. Jia, Z.I. Bashir, G.L. Collingridge, and E. Molnár. 2009. Tyrosine dephosphorylation regulates AMPAR internalisation in mGluR-LTD. *Mol. Cell. Neurosci.* 40:267–279. http://dx.doi.org/10.1016/j.mcn.2008.10.014

Grassi, S., A. Tozzi, C. Costa, M. Tantucci, E. Colcelli, M. Scarduzio, P. Calabresi, and V.E. Pettorossi. 2011. Neural 17β-estradiol facilitates long-term potentiation in the hippocampal CA1 region. *Neuroscience.* 192:67–73. http://dx.doi.org/10.1016/j.neuroscience.2011.06.078

Greer, P.L., R. Hanayama, B.L. Bloodgood, A.R. Mardinly, D.M. Lipton, S.W. Flavell, T.K. Kim, E.C. Griffith, Z. Waldon, R. Maehr, et al. 2010. The Angelman Syndrome protein Ube3A regulates synapse development by ubiquitinating arc. *Cell.* 140:704–716. http://dx.doi.org/10.1016/j.cell.2010.01.026

Hagena, H., and D. Manahan-Vaughan. 2011. Learning-facilitated synaptic plasticity at CA3 mossy fiber and commissural-associational synapses reveals different roles in information processing. *Cereb. Cortex.* 21:2442–2449. http://dx.doi.org/10.1093/cercor/bhq271

Hammond, R., R. Mauk, D. Ninaci, D. Nelson, and R.B. Gibbs. 2009. Chronic treatment with estrogen receptor agonists restores acquisition of a spatial learning task in young ovariectomized rats. *Horm. Behav.* 56:309–314. http://dx.doi.org/10.1016/j.yhbeh.2009.06.008

Hammond, R., D. Nelson, and R.B. Gibbs. 2011. GPR30 co-localizes with cholinergic neurons in the basal forebrain and enhances potassium-stimulated acetylcholine release in the hippocampus. *Psychoneuroendocrinology.* 36:182–192. http://dx.doi.org/10.1016/j.psyneuen.2010.07.007

Hammond, R., D. Nelson, E. Kline, and R.B. Gibbs. 2012. Chronic treatment with a GPR30 antagonist impairs acquisition of a spatial learning task in young female rats. *Horm. Behav.* 62:367–374. http://dx.doi.org/10.1016/j.yhbeh.2012.07.004

Hawley, W.R., E.M. Grissom, N.M. Moody, G.P. Dohanich, and N. Vasudevan. 2014. Activation of G-protein-coupled receptor 30 is sufficient to enhance spatial recognition memory in ovariectomized rats. *Behav. Brain Res.* 262:68–73. http://dx.doi.org/10.1016/j.bbr.2014.01.006

He, K., L. Song, L.W. Cummings, J. Goldman, R.L. Huganir, and H.K. Lee. 2009. Stabilization of Ca^{2+}-permeable AMPA receptors at perisynaptic sites by GluR1-S845 phosphorylation. *Proc. Natl. Acad. Sci. USA.* 106:20033–20038. http://dx.doi.org/10.1073/pnas.0910338106

Hojo, Y., T.A. Hattori, T. Enami, A. Furukawa, K. Suzuki, H.T. Ishii, H. Mukai, J.H. Morrison, W.G. Janssen, S. Kominami, et al. 2004. Adult male rat hippocampus synthesizes estradiol from pregnenolone by cytochromes P45017α and P450 aromatase localized in neurons. *Proc. Natl. Acad. Sci. USA.* 101:865–870. http://dx.doi.org/10.1073/pnas.2630225100

Hojo, Y., S. Higo, S. Kawato, Y. Hatanaka, Y. Ooishi, G. Murakami, H. Ishii, Y. Komatsuzaki, M. Ogiue-Ikeda, H. Mukai, and T. Kimoto. 2011. Hippocampal synthesis of sex steroids and corticosteroids: essential for modulation of synaptic plasticity. *Front. Endocrinol. (Lausanne).* 2:43.

Hosokawa, T., D. Mitsushima, R. Kaneko, and Y. Hayashi. 2015. Stoichiometry and phosphoisotypes of hippocampal AMPA-type glutamate receptor phosphorylation. *Neuron.* 85:60–67. http://dx.doi.org/10.1016/j.neuron.2014.11.026

Hou, L., and E. Klann. 2004. Activation of the phosphoinositide 3-kinase-Akt-mammalian target of rapamycin signaling pathway is required for metabotropic glutamate receptor-dependent long-term depression. *J. Neurosci.* 24:6352–6361. http://dx.doi.org/10.1523/JNEUROSCI.0995-04.2004

Hou, L., M.D. Antion, D. Hu, C.M. Spencer, R. Paylor, and E. Klann. 2006. Dynamic translational and proteasomal regulation of fragile X mental retardation protein controls mGluR-dependent long-term depression. *Neuron.* 51:441–454. http://dx.doi.org/10.1016/j.neuron.2006.07.005

Hsieh, Y.C., H.P. Yu, M. Frink, T. Suzuki, M.A. Choudhry, M.G. Schwacha, and I.H. Chaudry. 2007. G protein-coupled receptor 30-dependent protein kinase A pathway is critical in nongenomic effects of estrogen in attenuating liver injury after trauma-hemorrhage. *Am. J. Pathol.* 170:1210–1218. http://dx.doi.org/10.2353/ajpath.2007.060883

Jourdi, H., Y.T. Hsu, M. Zhou, Q. Qin, X. Bi, and M. Baudry. 2009. Positive AMPA receptor modulation rapidly stimulates BDNF release and increases dendritic mRNA translation. *J. Neurosci.* 29:8688–8697. http://dx.doi.org/10.1523/JNEUROSCI.6078-08.2009

Kase, H., K. Iwahashi, S. Nakanishi, Y. Matsuda, K. Yamada, M. Takahashi, C. Murakata, A. Sato, and M. Kaneko. 1987. K-252 compounds, novel and potent inhibitors of protein kinase C and cyclic nucleotide-dependent protein kinases. *Biochem. Biophys. Res. Commun.* 142:436–440. http://dx.doi.org/10.1016/0006-291X(87)90293-2

Kramár, E.A., L.Y. Chen, N.J. Brandon, C.S. Rex, F. Liu, C.M. Gall, and G. Lynch. 2009. Cytoskeletal changes underlie estrogen's acute effects on synaptic transmission and plasticity. *J. Neurosci.* 29:12982–12993. http://dx.doi.org/10.1523/JNEUROSCI.3059-09.2009

Kramár, E.A., A.H. Babayan, C.M. Gall, and G. Lynch. 2013. Estrogen promotes learning-related plasticity by modifying the synaptic cytoskeleton. *Neuroscience.* 239:3–16. http://dx.doi.org/10.1016/j.neuroscience.2012.10.038

Kühnle, S., B. Mothes, K. Matentzoglu, and M. Scheffner. 2013. Role of the ubiquitin ligase E6AP/UBE3A in controlling levels of the synaptic protein Arc. *Proc. Natl. Acad. Sci. USA.* 110:8888–8893. http://dx.doi.org/10.1073/pnas.1302792110

Lee, H.K., M. Barbarosie, K. Kameyama, M.F. Bear, and R.L. Huganir. 2000. Regulation of distinct AMPA receptor phosphorylation sites during bidirectional synaptic plasticity. *Nature.* 405:955–959. http://dx.doi.org/10.1038/35016089

Lee, B.H., M.J. Lee, S. Park, D.C. Oh, S. Elsasser, P.C. Chen, C. Gartner, N. Dimova, J. Hanna, S.P. Gygi, et al. 2010. Enhancement of proteasome activity by a small-molecule inhibitor of USP14. *Nature.* 467:179–184. http://dx.doi.org/10.1038/nature09299

Liu, Y., Q.X. Zhou, Y.Y. Hou, B. Lu, C. Yu, J. Chen, Q.L. Ling, J. Cao, Z.Q. Chi, L. Xu, and J.G. Liu. 2012. Actin polymerization-dependent increase in synaptic Arc/Arg3.1 expression in the amygdala is crucial for the expression of aversive memory associated with drug withdrawal. *J. Neurosci.* 32:12005–12017. http://dx.doi.org/10.1523/JNEUROSCI.0871-12.2012

Luine, V.N. 2008. Sex steroids and cognitive function. *J. Neuroendocrinol.* 20:866–872. http://dx.doi.org/10.1111/j.1365-2826.2008.01710.x

Mårtensson, U.E., S.A. Salehi, S. Windahl, M.F. Gomez, K. Swärd, J. Daszkiewicz-Nilsson, A. Wendt, N. Andersson, P. Hellstrand, P.O. Grände, et al. 2009. Deletion of the G protein-coupled receptor 30 impairs glucose tolerance, reduces bone growth, increases blood pressure, and eliminates estradiol-stimulated insulin release in female mice. *Endocrinology.* 150:687–698. http://dx.doi.org/10.1210/en.2008-0623

Matsuda, K., H. Sakamoto, H. Mori, K. Hosokawa, A. Kawamura, M. Itose, M. Nishi, E.R. Prossnitz, and M. Kawata. 2008. Expression and intracellular distribution of the G protein-coupled receptor 30 in rat hippocampal formation. *Neurosci. Lett.* 441:94–99. http://dx.doi.org/10.1016/j.neulet.2008.05.108

Mukai, H., T. Tsurugizawa, G. Murakami, S. Kominami, H. Ishii, M. Ogiue-Ikeda, N. Takata, N. Tanabe, A. Furukawa, Y. Hojo, et al. 2007. Rapid modulation of long-term depression and spinogenesis via synaptic estrogen receptors in hippocampal principal neurons. *J. Neurochem.* 100:950–967. http://dx.doi.org/10.1111/j.1471-4159.2006.04264.x

Murakami, G., Y. Hojo, M. Ogiue-Ikeda, H. Mukai, P. Chambon, K. Nakajima, Y. Ooishi, T. Kimoto, and S. Kawato. 2015. Estrogen receptor KO mice study on rapid modulation of spines and long-term depression in the hippocampus. *Brain Res.* 1621:133–146. http://dx.doi.org/10.1016/j.brainres.2014.12.002

Patrick, G.N., B. Bingol, H.A. Weld, and E.M. Schuman. 2003. Ubiquitin-mediated proteasome activity is required for agonist-induced endocytosis of GluRs. *Curr. Biol.* 13:2073–2081. http://dx.doi.org/10.1016/j.cub.2003.10.028

Patterson, S.L., C. Pittenger, A. Morozov, K.C. Martin, H. Scanlin, C. Drake, and E.R. Kandel. 2001. Some forms of cAMP-mediated long-lasting potentiation are associated with release of BDNF and nuclear translocation of phospho-MAP kinase. *Neuron.* 32:123–140. http://dx.doi.org/10.1016/S0896-6273(01)00443-3

Peebles, C.L., J. Yoo, M.T. Thwin, J.J. Palop, J.L. Noebels, and S. Finkbeiner. 2010. Arc regulates spine morphology and maintains network stability in vivo. *Proc. Natl. Acad. Sci. USA.* 107:18173–18178. http://dx.doi.org/10.1073/pnas.1006546107

Prossnitz, E.R., J.B. Arterburn, H.O. Smith, T.I. Oprea, L.A. Sklar, and H.J. Hathaway. 2008. Estrogen signaling through the transmembrane G protein-coupled receptor GPR30. *Annu. Rev. Physiol.* 70:165–190. http://dx.doi.org/10.1146/annurev.physiol.70.113006.100518

Rial Verde, E.M., J. Lee-Osbourne, P.F. Worley, R. Malinow, and H.T. Cline. 2006. Increased expression of the immediate-early gene arc/arg3.1 reduces AMPA receptor-mediated synaptic transmission. *Neuron.* 52:461–474. http://dx.doi.org/10.1016/j.neuron.2006.09.031

Roberts, L.A., M.J. Higgins, C.T. O'Shaughnessy, T.W. Stone, and B.J. Morris. 1996. Changes in hippocampal gene expression associated with the induction of long-term potentiation. *Brain Res. Mol. Brain Res.* 42:123–127. http://dx.doi.org/10.1016/S0169-328X(96)00148-9

Rüegg, U.T., and G.M. Burgess. 1989. Staurosporine, K-252 and UCN-01: potent but nonspecific inhibitors of protein kinases. *Trends Pharmacol. Sci.* 10:218–220. http://dx.doi.org/10.1016/0165-6147(89)90263-0

Ruiz-Palmero, I., M. Hernando, L.M. Garcia-Segura, and M.A. Arevalo. 2013. G protein-coupled estrogen receptor is required for the neuritogenic mechanism of 17β-estradiol in developing hippocampal neurons. *Mol. Cell. Endocrinol.* 372:105–115. http://dx.doi.org/10.1016/j.mce.2013.03.018

Santos, A.R., M. Mele, S.H. Vaz, B. Kellermayer, M. Grimaldi, M. Colino-Oliveira, D.M. Rombo, D. Comprido, A.M. Sebastião, and C.B. Duarte. 2015. Differential role of the proteasome in the early and late phases of

BDNF-induced facilitation of LTP. *J. Neurosci.* 35:3319–3329. http://dx.doi.org/10.1523/JNEUROSCI.4521-14.2015

Sato, K., T. Akaishi, N. Matsuki, Y. Ohno, and K. Nakazawa. 2007. β-Estradiol induces synaptogenesis in the hippocampus by enhancing brain-derived neurotrophic factor release from dentate gyrus granule cells. *Brain Res.* 1150:108–120. http://dx.doi.org/10.1016/j.brainres.2007.02.093

Schägger, H. 2006. Tricine-SDS-PAGE. *Nat. Protoc.* 1:16–22. http://dx.doi.org/10.1038/nprot.2006.4

Scharfman, H.E., and N.J. MacLusky. 2014. Differential regulation of BDNF, synaptic plasticity and sprouting in the hippocampal mossy fiber pathway of male and female rats. *Neuropharmacology.* 76:696–708. http://dx.doi.org/10.1016/j.neuropharm.2013.04.029

Scharfman, H.E., T.C. Mercurio, J.H. Goodman, M.A. Wilson, and N.J. MacLusky. 2003. Hippocampal excitability increases during the estrous cycle in the rat: a potential role for brain-derived neurotrophic factor. *J. Neurosci.* 23:11641–11652.

Shiroma, S., T. Yamaguchi, and K. Kometani. 2005. Effects of 17β-estradiol on chemically induced long-term depression. *Neuropharmacology.* 49:97–102. http://dx.doi.org/10.1016/j.neuropharm.2005.02.002

Sivakumaran, S., M.H. Mohajerani, and E. Cherubini. 2009. At immature mossy-fiber-CA3 synapses, correlated presynaptic and postsynaptic activity persistently enhances GABA release and network excitability via BDNF and cAMP-dependent PKA. *J. Neurosci.* 29:2637–2647. http://dx.doi.org/10.1523/JNEUROSCI.5019-08.2009

Spencer-Segal, J.L., M.C. Tsuda, L. Mattei, E.M. Waters, R.D. Romeo, T.A. Milner, B.S. McEwen, and S. Ogawa. 2012. Estradiol acts via estrogen receptors alpha and beta on pathways important for synaptic plasticity in the mouse hippocampal formation. *Neuroscience.* 202:131–146. http://dx.doi.org/10.1016/j.neuroscience.2011.11.035

Srivastava, D.P., and P.D. Evans. 2013. G-protein oestrogen receptor 1: trials and tribulations of a membrane oestrogen receptor. *J. Neuroendocrinol.* 25:1219–1230. http://dx.doi.org/10.1111/jne.12071

Srivastava, D.P., K.M. Woolfrey, K.A. Jones, C.Y. Shum, L.L. Lash, G.T. Swanson, and P. Penzes. 2008. Rapid enhancement of two-step wiring plasticity by estrogen and NMDA receptor activity. *Proc. Natl. Acad. Sci. USA.* 105:14650–14655. (published erratum appears in *Proc. Natl. Acad. Sci. USA*. 2008. 105:20045) http://dx.doi.org/10.1073/pnas.0801581105

Srivastava, D.P., K.M. Woolfrey, and P. Penzes. 2013. Insights into rapid modulation of neuroplasticity by brain estrogens. *Pharmacol. Rev.* 65:1318–1350. http://dx.doi.org/10.1124/pr.111.005272

Steward, O., C.S. Wallace, G.L. Lyford, and P.F. Worley. 1998. Synaptic activation causes the mRNA for the IEG Arc to localize selectively near activated postsynaptic sites on dendrites. *Neuron.* 21:741–751. http://dx.doi.org/10.1016/S0896-6273(00)80591-7

Sun, J., Y. Liu, S. Moreno, M. Baudry, and X. Bi. 2015. Imbalanced mechanistic target of rapamycin C1 and C2 activity in the cerebellum of Angelman syndrome mice impairs motor function. *J. Neurosci.* 35:4706–4718. http://dx.doi.org/10.1523/JNEUROSCI.4276-14.2015

Taniguchi, N., Y. Shinoda, N. Takei, H. Nawa, A. Ogura, and K. Tominaga-Yoshino. 2006. Possible involvement of BDNF release in long-lasting synapse formation induced by repetitive PKA activation. *Neurosci. Lett.* 406:38–42. http://dx.doi.org/10.1016/j.neulet.2006.06.071

Waters, E.M., L.I. Thompson, P. Patel, A.D. Gonzales, H.Z. Ye, E.J. Filardo, D.J. Clegg, J. Gorecka, K.T. Akama, B.S. McEwen, and T.A. Milner. 2015. G-protein-coupled estrogen receptor 1 is anatomically positioned to modulate synaptic plasticity in the mouse hippocampus. *J. Neurosci.* 35:2384–2397. http://dx.doi.org/10.1523/JNEUROSCI.1298-14.2015

Waung, M.W., B.E. Pfeiffer, E.D. Nosyreva, J.A. Ronesi, and K.M. Huber. 2008. Rapid translation of Arc/Arg3.1 selectively mediates mGluR-dependent LTD through persistent increases in AMPAR endocytosis rate. *Neuron.* 59:84–97. http://dx.doi.org/10.1016/j.neuron.2008.05.014

Widagdo, J., Y.J. Chai, M.C. Ridder, Y.Q. Chau, R.C. Johnson, P. Sah, R.L. Huganir, and V. Anggono. 2015. Activity-dependent ubiquitination of GluA1 and GluA2 regulates AMPA receptor intracellular sorting and degradation. *Cell Reports.* 10:783–795. http://dx.doi.org/10.1016/j.celrep.2015.01.015

Woolley, C.S., E. Gould, M. Frankfurt, and B.S. McEwen. 1990. Naturally occurring fluctuation in dendritic spine density on adult hippocampal pyramidal neurons. *J. Neurosci.* 10:4035–4039.

Yuen, E.Y., J. Wei, W. Liu, P. Zhong, X. Li, and Z. Yan. 2012. Repeated stress causes cognitive impairment by suppressing glutamate receptor expression and function in prefrontal cortex. *Neuron.* 73:962–977. http://dx.doi.org/10.1016/j.neuron.2011.12.033

Zadran, S., Q. Qin, X. Bi, H. Zadran, Y. Kim, M.R. Foy, R. Thompson, and M. Baudry. 2009. 17-β-estradiol increases neuronal excitability through MAP kinase-induced calpain activation. *Proc. Natl. Acad. Sci. USA.* 106:21936–21941. http://dx.doi.org/10.1073/pnas.0912558106

Zucchetti, A.E., I.R. Barosso, A.C. Boaglio, C.L. Basiglio, G. Miszczuk, M.C. Larocca, M.L. Ruiz, C.A. Davio, M.G. Roma, F.A. Crocenzi, and E.J. Pozzi. 2014. G-protein-coupled receptor 30/adenylyl cyclase/protein kinase A pathway is involved in estradiol 17ß-D-glucuronide-induced cholestasis. *Hepatology.* 59:1016–1029. http://dx.doi.org/10.1002/hep.26752